

Role of Laser Beam Geometry in Improving Implosion Symmetry and Performance for Indirect- Drive Inertial Confinement Fusion

*R.E. Turner, P.A. Amendt, O.L. Landen, L.J. Suter, R.J.
Wallace, and B.A. Hammel*

This article was submitted to Physical Review Letters

U.S. Department of Energy

Lawrence
Livermore
National
Laboratory

June 17, 2002

Role of laser beam geometry in improving implosion symmetry and performance for indirect-drive inertial confinement fusion

R. E. Turner, P. A. Amendt, O. L. Landen, L. J. Suter, R. J. Wallace,
and B. A. Hammel

Lawrence Livermore National Laboratory, P.O. Box 808, Livermore, California 94550

(Received 20 January 2003; accepted 28 March 2003)

The role of a high-Z radiation cavity or hohlraum in inertial confinement fusion is to convert laser energy into soft x-ray energy, in a highly spatially symmetric manner, so that a centrally located capsule containing deuterium and tritium can be uniformly imploded. In practice, however, the asymmetry introduced by the small number of high intensity laser beams can introduce significant perturbations in the drive uniformity. Experiments performed on Nova (10 beams) [J. T. Hunt and D. R. Speck, *Opt. Eng.* **28**, 461 (1989)] and Omega (using 40 beams) [J. M. Sources, R. L. McCrory, C. P. Verdon *et al.*, *Phys. Plasmas* **3**, 2108 (1996)] demonstrate a significant improvement in symmetry and target performance from a fourfold increase in the number of laser beams. © 2003 American Institute of Physics. [DOI: 10.1063/1.1576762]

I. INTRODUCTION

In indirectly driven inertial confinement fusion (ICF), laser energy is directed into a cylindrical cavity constructed of high atomic number materials. The laser energy is absorbed and efficiently reradiated; as the cavity walls heat, their reradiated fraction of x rays (or albedo) can approach one, and the radiation within the cavity becomes very spatially symmetric, especially at high spatial frequencies.¹ The radiation from the walls and laser hot spots is absorbed by, and ablates, the surface of the capsule containing the deuterium fuel; the ablation pressure then implodes the remaining capsule wall and fuel. However, the regions where laser energy is deposited (“hot spots”) remain hotter than the indirectly heated walls, while the pair of holes where the laser beams enter the hohlraum produce little or no radiation. These residual asymmetries in the radiation flux incident on the capsule can lead to asynchronous shock convergence at the capsule’s center and asymmetric implosions. For example, it has been calculated^{2,3} that to achieve ignition and generate significant fusion yield on the National Ignition Facility,⁴ it will be necessary to maintain drive flux asymmetries at the capsule to less than 2% time-averaged and less than 10% over any 10% epoch in the drive.

II. RESULTS

It is convenient to examine the drive symmetry on the capsule in terms of spherical harmonics $Y_{\ell,m}(\theta, \phi)$ where the polar angle theta is measured from the cylindrical hohlraum symmetry axis (see Fig. 1). We thus speak of Legendre “ ℓ ” modes, and azimuthal “ m ” modes. To illustrate the importance of beam geometry, we show here the improvements in hohlraum symmetry and implosion performance by switching from 10 beam Nova⁵ laser illumination to 40 beam Omega⁶ laser illumination.

The Nova hohlraum geometry consisted of 5 beams, arranged in a ring, entering each end of the hohlraum at 50° to

the symmetry axis [Fig. 1(a)]. Due to the presumed left–right symmetry, only even ℓ modes appeared intrinsically. Thus the lowest order modes were $\ell=2$, and $m=5$. Although the laser entrance holes also impose an $\ell=2$ perturbation on the drive, it was possible to position the ring of beams in a location where the $\ell=2$ perturbation is zeroed out.⁷ Thus the lowest remaining uncontrolled modes were $\ell=4$ and $m=5$. Since the hohlraum walls expand inward with time, the laser beam absorption region will move and thus only a properly weighted time-averaged value of the $\ell=2$ mode can be zeroed, so as to ensure the final implosion shape is round. However, time-averaged symmetry, by itself, is not sufficient for achieving high fusion yields as the convergence of the sequentially launched, stronger shocks, which are required to form the hot spot ignition, will be distorted by time-dependent asymmetries. In particular, the Nova-type single ring per side illumination geometry leads to >20% time-dependent excursions in the $\ell=2$ mode [Fig. 1(c)] which would thwart ignition at the NIF.

In contrast, cylindrical hohlraums at the Omega facility can be illuminated by 20 laser beams at each end, which can be arranged⁸ in 3 rings of 5, 5, and 10 beams at incidence angles of 21°, 42°, and 59° [Fig. 1(b)]. The multiple rings allow time-averaged control of both $\ell=2$ and $\ell=4$ modes. Furthermore, due to the interleaving of the beams in azimuth, the lowest natural azimuthal mode is $m=10$ for the inner ring and $m=15$ for the outer rings. In addition, this illumination geometry provides better symmetry isolation from time-dependent changes such as wall motion. This can be understood qualitatively by noting that for a single pair of rings of beams, as at Nova, the variation in the $\ell=2$ moment with beam pointing is greatest at the point where the beams are pointed, the $\ell=2$ node, whereas for the Omega configuration, with multiple rings of beams, the rings are at locations closer to the $\ell=2$ antinodes (of opposite sign) where the $\ell=2$ asymmetry changes more slowly with beam position changes.⁹ Figures 1(c) and 1(d) show results from two-

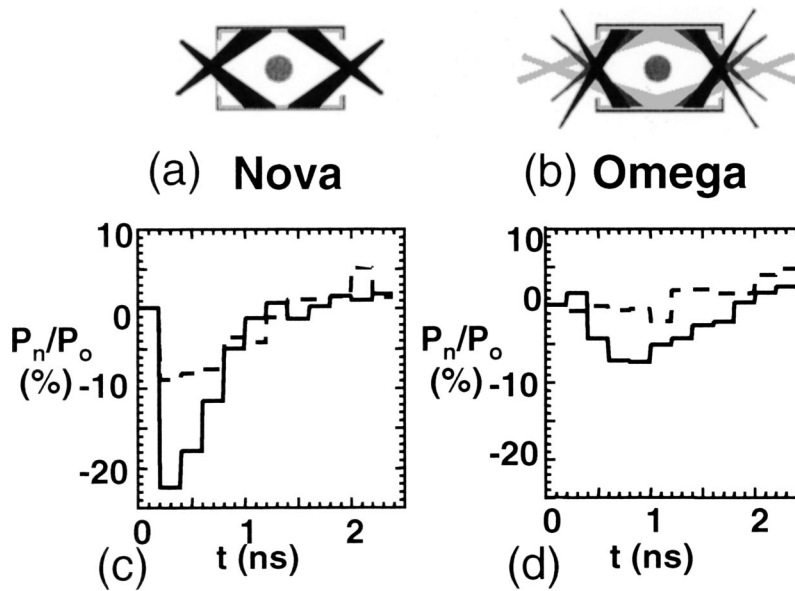


FIG. 1. Schematic of cylindrical hohlraum illumination geometry for (a) 10 beam Nova and (b) 40 beams of Omega. Below each schematic are comparison of calculated $\ell=2$ mode (solid line) and $\ell=4$ (dashed line) mode flux asymmetries at capsule for (c) single ring per side Nova vs (d) multiple ring per side Omega hohlraum illumination geometries, expressed as a percentage of the zero order flux.

dimensional (2D) radiation hydrodynamics simulations of the $\ell=2$ and $\ell=4$ time-dependent capsule ablation pressure asymmetries for the Nova and Omega hohlraum illumination geometries used in the experiments. The hohlraums are 1.6 mm in diameter by 2.4 mm long with 1.2 mm diameter laser entrance holes. The hohlraums are driven by a 2-step 6:1 contrast, 2.5 ns long laser pulse¹⁰ with up to 30 (15) kJ available in the Nova (Omega) geometry. The beam pointing in each case has been optimized to provide zero time-integrated $\ell=2$ asymmetry at the capsule, as well as zero time-integrated $\ell=4$ for the multiple ring case. The Omega geometry is predicted to provide $3\times$ smaller asymmetry swings in time for the $\ell=2$ and 4 modes.

We have validated these predicted improvements in the low-order drive asymmetries using two complementary techniques. The first technique replaces the implosion capsule with a low density foam ball surrogate,^{11,12} with the low density used to amplify the effects of flux asymmetries. The x-ray drive shock-compresses the foam, whose limb distortion from round can be imaged at various times by x-ray backlighting to provide time-dependent asymmetry information. The foam balls used were 400 μm diameter, 0.3 g/cm^3 SiO_2 balls backlit by 4.7 keV x rays produced by a noninvasive external laser-plasma Ti source. Up to 8 images were recorded in 100 ps steps with 10 μm , 70 ps resolution.

Figures 2(a) and 2(b) show the measured $\ell=2$ and 4 components of the foam ball images as a function of time. Overplotted are the calculated distortions as postprocessed from 2D radiation-hydrodynamics simulations. The measured and calculated departures from symmetry are $<2 \mu\text{m}$

at all times, as predicted by simulations. Specifically, the maximum $\ell=2$ and 4 flux asymmetries inferred from these sequences of images is $<5\%/ns$, a factor-of-2 better than required for ignition. In comparison to this multiple ring data, the single ring Nova data show [Fig. 2(c)] an $l=2$ swing of nearly 4 μm for the optimized (net swing of zero) case.¹² Furthermore, Fig. 2(c) shows that the $\ell=4$ component from an Omega experiment¹³ with the beams all in one ring per side (hence, absent $l=4$ control) is $3\times$ larger.

The second technique, “symmetry capsules” (Refs. 13 and 14), records the shape of x-ray emission images at peak compression to infer time-integrated asymmetry. The capsules used were 440- μm -diameter, 32 μm -thick plastic shells with 1% Ge-dopant to control x-ray preheat. Additionally, the targets were filled with 50 atm of D_2 , and doped with 0.05–0.1 atm Ar for increased visibility of hard x-ray emission at peak compression. The 4–6 keV emission from the cores was imaged with 5–10 μm resolution by pinhole arrays onto 70 ps gated cameras. Figure 3 shows the measured image core ellipticity (ratio of vertical to horizontal FWHM, a simplified measure of the effect of lowest order asymmetries) as a function of the implosion convergence ratio. The core distortions lie within that expected for $\pm 2\%$ excursions in $\ell=2$ time-integrated drive asymmetry, demonstrating repeatable control of this asymmetry to the level required for ignition on the NIF.

As a test of whether improvements in symmetry can lead to improvements in implosion performance, we also compare the D_2 neutron yields from these indirectly driven capsules with simulations. The modeling matches the measured radia-

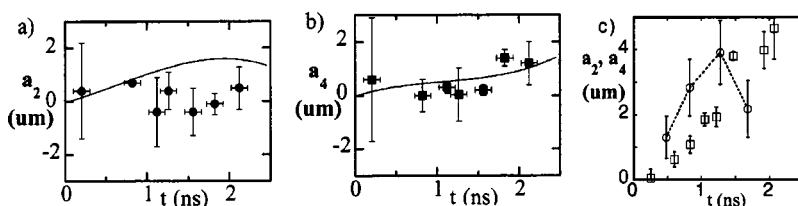


FIG. 2. (a) $\ell=2$ and (b) $\ell=4$ mode distortions of foam balls vs time. Solid symbols are multiple ring per side Omega data, and the solid line is simulation. (c) Single ring per side data: open circles (connected with dashed line) are $l=2$ Nova data; squares are $l=4$ Omega data.

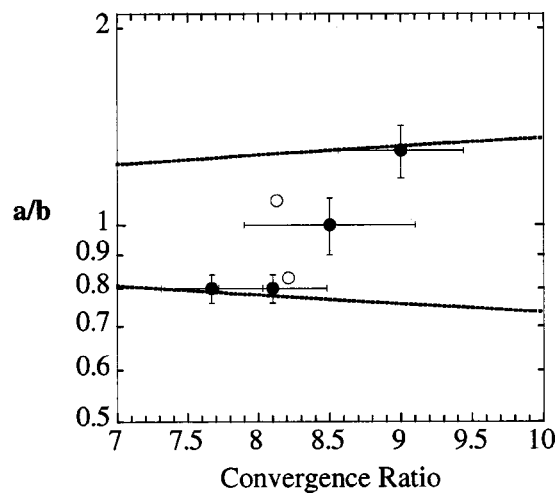


FIG. 3. Measured (solid symbols) core image ellipticities vs convergence ratio. Open symbols are simulation results. Overplotted (dashed lines) is expected ellipticity for $\pm 2\%$ average $\ell=2$ flux asymmetry.

tion drive history of the hohlraums on both Nova¹⁰ and Omega,¹⁵ with peak radiation temperatures of 200 eV. The Nova modeling included a 10% measured laser backscatter loss. For the Omega simulations, we assumed laser backscatter losses to be negligible due to the improved beam quality.

Measurements on representative beams from all 3 laser cones showed the laser backscatter to be $<3\%$ of the incident energy, making this a reasonable assumption.

Figure 4 shows the measured D_2 neutron yield, divided by the (1D) calculated yield, as a function of the experimentally inferred convergence ratio for both the older 10 beam Nova data^{10,16} and the 40 beam Omega data. The convergence ratio is inferred by measuring secondary (DT) neutrons; the ratio of DT/DD neutrons provides a measure of the fuel radius-density (ρR) product.¹⁷ By assuming conservation of mass, we deduce the convergence ratio. Since this is a spatially averaged measurement, the relatively small asymmetries reported here are insufficient to produce measurable

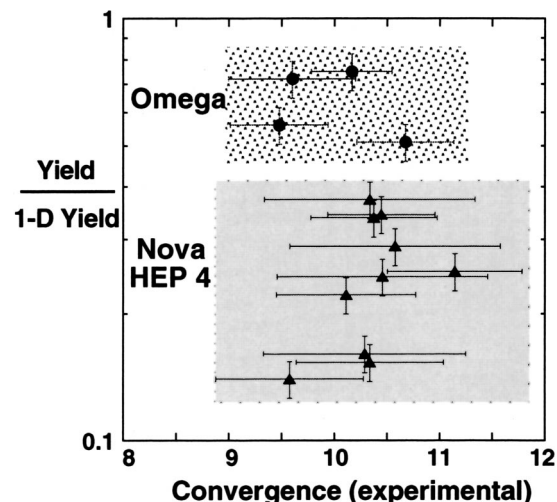


FIG. 4. Comparison of measured yield normalized to calculated 1D clean yield vs measured convergence ratio for implosions driven by single ring per side Nova (triangles) vs multiple ring per side Omega (circles) hohlraums.

TABLE I. Measured DD neutron yields and convergences, and ratio of measured yields to calculated yields, for Omega experiments.

Experimental DD neutron yield (units of 10^8 neutrons)	Experimental convergence	Ratio of experimental to calculated (1D) yield
5.27	9.6	0.72
10.4	10.2	0.75
8.73	10.7	0.51
11.2	9.5	0.56

differences in the convergence measurement. The Omega hohlraums provide a greater than $2\times$ improvement in implosion performance relative to 1D expectations. The measured values of the DD neutron yields for the Omega experiments are tabulated in Table I. An additional experiment was performed on Nova, using Omega-like energy levels (15.7 kJ) to verify that the $2\times$ laser energy difference between the two facilities is not the source of the difference in implosion performance. This experiment produced an experimental yield of 2×10^8 , noticeably smaller than the Omega yields in Table I. The resulting yield/calculated yield for this shot is 0.18, similar to the other Nova data shown in Fig. 4. 2D and 3D calculations indicate¹⁸ that, for these low-convergence capsules, the $\ell=2$ and 4 and $m=5$ drive asymmetries present on Nova are sufficient to reduce the neutron yield by $2\times$ ($\ell=2,4$ modes) and 10% ($m=5$ mode) compared to 1D simulations, without invoking any additional hydrodynamic instability growth of capsule imperfections (rms surface roughness $<0.03\ \mu\text{m}$). By contrast, the predicted yield degradation due to residual intrinsic and random flux asymmetry for the Omega implosions is $<5\%$ for the convergence ≈ 10 capsules. A further 10%–20% yield degradation is estimated to occur from surface roughness-induced mix and low-order ($\ell=1,2$) shell perturbations.

III. CONCLUSIONS

In summary, we have presented experimental evidence that low order asymmetries, due to the finite number of laser beams, limited the performance of even low convergence capsules on the 10 beam Nova system. In contrast, the 40 beams available on Omega have enabled us to demonstrate time-resolved asymmetry swings of less than 5%/ns, as required for ignition on the NIF, and repeatable, near 1D calculated implosion performance.

ACKNOWLEDGMENT

This work was performed under the auspices of the U.S. Department of Energy by the University of California Lawrence Livermore National Laboratory under Contract No. W-7405-Eng-48.

¹A. Caruso and C. Strangio, Jpn. J. Appl. Phys., Part 1 **30**, 1095 (1991); M. Murakami and J. Meyer-ter-Vehn, Nucl. Fusion **31**, 1333 (1991).

²J. D. Lindl, Phys. Plasmas **2**, 3933 (1995).

³S. W. Haan, S. M. Pollaine, J. D. Lindl *et al.*, Phys. Plasmas **2**, 2480 (1995).

⁴J. A. Paisner, J. D. Boyes, S. A. Kumpan, W. H. Lowdermilk, and M. S. Sorem, Laser Focus World **30**, 75 (1994).

- ⁵J. T. Hunt and D. R. Speck, *Opt. Eng.* **28**, 461 (1989).
- ⁶J. M. Soares, R. L. McCrory, C. P. Verdon *et al.*, *Phys. Plasmas* **3**, 2108 (1996).
- ⁷L. J. Suter, A. A. Hauer, L. V. Powers *et al.*, *Phys. Rev. Lett.* **73**, 2328 (1994).
- ⁸T. J. Murphy, J. M. Wallace, N. D. Delamater *et al.*, *Phys. Rev. Lett.* **81**, 108 (1998).
- ⁹O. L. Landen, P. A. Amendt, L. J. Suter *et al.*, *Phys. Plasmas* **6**, 2137 (1999).
- ¹⁰O. L. Landen, C. J. Keane, B. A. Hammel *et al.*, *Phys. Plasmas* **3**, 2094 (1996).
- ¹¹P. Amendt, S. G. Glendinning, B. A. Hammel *et al.*, *Phys. Plasmas* **4**, 1862 (1997).
- ¹²S. G. Glendinning, P. Amendt, B. D. Cline *et al.*, *Rev. Sci. Instrum.* **70**, 536 (1999).
- ¹³R. E. Turner, P. Amendt, O. L. Landen *et al.*, *Phys. Plasmas* **7**, 333 (2000).
- ¹⁴A. A. Hauer, L. Suter, N. Delamater *et al.*, *Phys. Plasmas* **2**, 2488 (1995); N. D. Delamater, T. J. Murphy, A. A. Hauer *et al.*, *ibid.* **3**, 2022 (1996).
- ¹⁵P. A. Amendt, R. E. Turner, and O. L. Landen, *Phys. Rev. Lett.* **89**, 165001 (2002).
- ¹⁶M. M. Marinak, R. E. Tipton, O. L. Landen *et al.*, *Phys. Plasmas* **3**, 2070 (1996).
- ¹⁷H. Azechi, N. Miyanaga, R. O. Stapf *et al.*, *Appl. Phys. Lett.* **49**, 555 (1986); M. D. Cable and S. P. Hatchett, *J. Appl. Phys.* **62**, 2233 (1987).
- ¹⁸M. M. Marinak, G. D. Kerbel, N. A. Gentile, O. Jones, S. Pollaine, T. R. Dittrich, and S. W. Haan, *Phys. Plasmas* **8**, 2275 (2001).